European Coordination for Accelerator Research and Development

PUBLICATION

Active Control of Quadrupole Motion for Future Linear Particle Colliders

Collette, Christophe (CERN) *et al*

28 May 2010

The research leading to these results has received funding from the European Commission under the FP7 Research Infrastructures project EuCARD, grant agreement no. 227579.

This work is part of EuCARD Work Package **9: Technology for normal conducting higher energy linear accelerators**.

The electronic version of this EuCARD Publication is available via the EuCARD web site <http://cern.ch/eucard> or on the CERN Document Server at the following URL : <http://cdsweb.cern.ch/record/1268422>

ACTIVE CONTROL OF QUADRUPOLE MOTION FOR FUTURE LINEAR PARTICLE COLLIDERS

C. Collette, K. Artoos, A. Kuzmin, M. Sylte, M. Guinchard, C. Hauviller
Engineering Department, European Organization for Nuclear Research
Geneva 23, 1211 Geneva, Switzerland
email: christophe.collette@cern.ch

ABSTRACT
The future Compact LInear particle Collider (CLIC) under study at CERN will require to stabilize heavy electromagnets, and also provide them some positioning capabilities. Firstly, this paper presents the concept adopted to address both requirements. Secondly, the control strategy adopted for the stabilization is studied on a single degree of freedom system, and validated experimentally in a quiet environment.

KEY WORDS
Seismic excitation, Stabilization, Position feedback, Precise positioning.

1 Introduction

In the Compact LInear Collider (CLIC) currently under study [1], electrons and positrons will be accelerated in two linear accelerators to collide at the interaction point with an energy of $0.5 - 3\ TeV$. To acquire such a high energy, the total length of the machine is expected to be up to $48\ km$. This linear accelerator will consist of a succession of accelerating structures and heavy electromagnets (quadrupoles). The former are used to accelerate the particles to increase their energy; the latter are used to maintain the beam inside the vacuum chamber (alternating gradient) and to reach the required luminosity at the collision point. However, any oscillation of one quadrupole deflects the beam, and reduces the luminosity. More precisely, if $\Phi_x(f)$ is the power spectral density of the vertical displacement of the quadrupole, it has been estimated that the integrated Root Mean Square (RMS) $\sigma_x(f)$, defined as

$$\sigma_x(f) = \sqrt{\int_f^\infty \Phi_x(\nu) d\nu} \qquad (1)$$

must stay below $1\ nm$ [2] above $1\ Hz$ to ensure sufficient performances (Fig.1(a)). Similarly, it must stay below $5\ nm$ in the lateral direction. This concerns about 2000 quadrupoles per beam line. Additionally, about 80 quadrupoles should have the capability to move by steps of some tens of nanometers every $20\ ms$ [3], with a precision of $+/-\ 1nm$ (see Fig.1(b)).
To demonstrate the feasibility to fulfil such stringent requirements, it is planned to build a mock-up of the longest

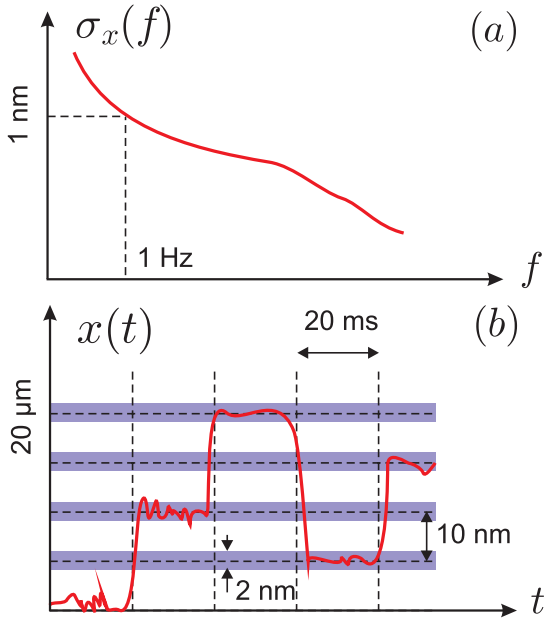

Figure 1. (a) Frequency domain requirements for the stabilization; (b) Time domain requirements for the positioning.

CLIC main beam quadrupole with its support.

2 Control strategy

The stabilization of structures at the nanometer scale is a concern in various fields of precision engineering, like interferometers [4], microscopes [5] or manufacturing [6]. In this section, only a few key experiments of quadrupole stabilization are presented, and some of their characteristics are compared in Table 1: the number of degrees of freedom (d.o.f.), the type of actuator, the number of stages for the isolation (i.e. the number of spring-mass systems in series), the positioning capability, the overall stiffness of the support and the ratio between the RMS integrated displacement of the ground and the mass to stabilize at $1\ Hz$.
In order to understand the advantages and disadvantages of these approaches, let us consider a single d.o.f. quadrupole shown in Fig. 2(a). Assuming that the alignment stage (which is not discussed in this paper) is completely rigid,

	DESY	CERN	LAPP	SLAC
Ref.	[7, 8]	[9]	[10]	[11, 12]
d.o.f.	1	1	1	6
Actuator	Piezo	Piezo	Piezo	Electro-static
Stages	1	2	2	1
Positioning	No	No	No	No
Suspension	Stiff	Soft	Soft	Soft
σ_w/σ_x@ 1 Hz	3	3	2	50

Table 1. Comparison of several strategies adopted for the stabilization of quadrupoles.

the transmissibility $T_{wx}(f)$ between the ground w and the mass (quadrupole) displacement x is shown in Fig. 2(b) for three values of the damping coefficient c. On the transmissibility, one sees that an overshoot appears at the resonance frequency of the system. The isolation properties of the support starts at $\sqrt{2}f_n$ (where $2\pi f_n = \sqrt{k/m}$). Above that frequency, the amplitude of the response is smaller than the amplitude of the excitation. Increasing the damper constant c leads to a reduction of the overshoot, but at the expense of a degradation of the isolation performances. On the other side, a reduction of the stiffness increases the isolation at low frequencies (Fig.3(a)). Then, in order to benefit from the passive isolation, the first idea is to reduce the value of f_n as much as possible. It has been shown [11, 12] that such a strategy can lead to a very high reduction of the RMS integrated (see the last column of Table 1). However, the main drawback is that, as the resonance frequency of the system decreases, it becomes more sensitive to any external force directly applied on the quadrupole at very low frequency. This is illustrated in Fig. 3(b), showing the transmissibility between a force F_a applied on the quadrupole and its vertical displacement x. Two stages configurations [9, 10] are also based on soft supports. While efficient for the stabilization of quadrupoles, these systems are much too soft to fulfil the positioning requirements (Fig. 1(b)). For this reason, it has been decided to use stiff supports like in [7, 8], and reduce actively the transmissibility $T_{wx}(f)$ at low frequencies (mainly the range between 1 Hz and 20 Hz) [13]. The next section presents the concept studied to support the six d.o.f. quadrupole. Then, this concept is studied in more details on a single d.o.f. system, and validated experimentally in a quiet environment.

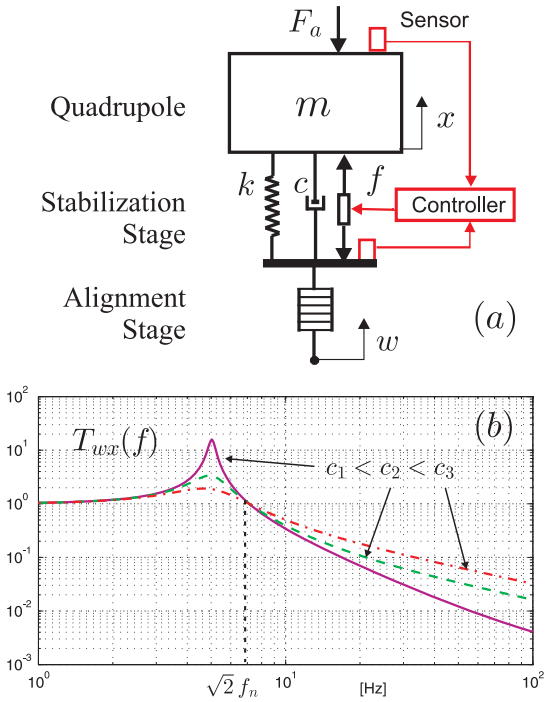

Figure 2. (a) Single d.o.f oscillator; (b) Transmissibility $T_{wx}(f)$ between the ground and the mass displacement for three values of the damping coefficient.

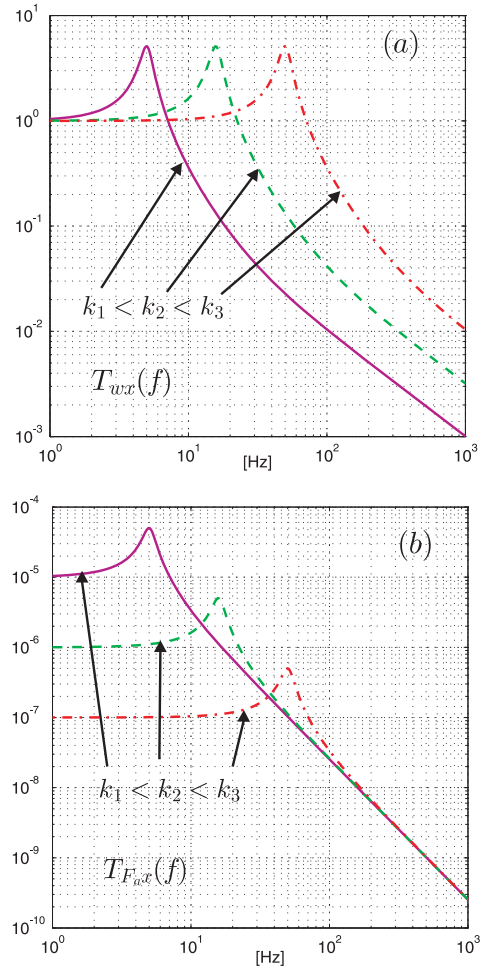

Figure 3. Effect of the support stiffness on (a) The transmissibility $T_{wx}(f)$ between the ground and the mass displacement; (b) The transmissibility $T_{F_a x}(f)$ between a force F_a applied on the mass and the mass displacement.

3 Six d.o.f. quadrupole

The strategy adopted to provide the required positioning capabilities to the quadrupole is inspired from the concept of a Stewart platform [14, 15, 16]. It is a well known concept that has been applied for both vibration isolation and precise positioning of ground and space structures. Because of the long size quadrupole, the six legs are mounted as depicted in Fig. 4. For reasons of simplicity, it has been decided to fix the orientations of the legs using only two parameters: α fix the orientation in the horizontal plane and β the inclination with respect to a vertical axis. Their numerical values result from a tradeoff between the following requirements: provide a good stability in the longitudinal direction, manoeuvrability in both vertical and lateral directions, allow a sufficient resolution in the vertical direction, and ensure a static equilibrium when no control is applied. Assuming that the quadrupole is rigid, and no damping in the legs, the dynamic equations of the system are

$$M\ddot{\mathbf{x}} + K\mathbf{x} = B\mathbf{f} + E\mathbf{w} \tag{2}$$

where M and K are the mass and stiffness matrices, $\mathbf{x} = (x, y, z, \theta, \phi, \psi)$ is the vector describing small displacements of the quadrupole, $\mathbf{f} = (f_1, f_2, ..., f_6)^T$ is the vector of active control forces in the six legs, $\mathbf{w}$ is the ground excitation vector, E is the excitation matrix and B is the force jacobian matrix expressing $\mathbf{f}$ in the frame of the quadrupole. M =diag$(m, m, m, I_\theta, I_\phi, I_\psi)$. Analytical expressions of K and B are found as follows. First, we know from [15] that the Jacobian matrix relating the elongations velocities of the legs $\mathbf{q}$ and the velocity vector $\dot{\mathbf{x}}$ as $\dot{\mathbf{q}} = J\dot{\mathbf{x}}$ is given by

$$J = \begin{pmatrix} \dots & \dots \\ \mathbf{1}_i^T & -\mathbf{1}_i^T \tilde{\mathbf{p}}_i \\ \dots & \dots \end{pmatrix} \tag{3}$$

where $\mathbf{p}_i$ is the position of the extremity of leg i, $\tilde{\mathbf{p}}_i$ is the antisymmetric matrix calculated from $\mathbf{p}_i$ and $\mathbf{1}_i$ is a unit vector in the direction of leg i. In details, the matrices of unit vector $Q = (\mathbf{1}_1, ..., \mathbf{1}_6)$ and positions of legs extremity $P = (\mathbf{p}_1^T, ..., \mathbf{p}_6^T)$ are respectively

$$Q = \begin{pmatrix} \sin\beta\cos\alpha & \sin\beta\sin\alpha & \cos\beta \\ -\sin\beta\cos\alpha & \sin\beta\sin\alpha & \cos\beta \\ -\sin\beta\sin\alpha & -\sin\beta\cos\alpha & \cos\beta \\ \sin\beta\sin\alpha & \sin\beta\cos\alpha & \cos\beta \\ \sin\beta\cos\alpha & -\sin\beta\sin\alpha & \cos\beta \\ -\sin\beta\cos\alpha & -\sin\beta\sin\alpha & \cos\beta \end{pmatrix}$$

and

$$P = \begin{pmatrix} -R & R & -R & R & -R & R \\ -L & -L & 0 & 0 & L & L \\ h & h & h & h & h & h \end{pmatrix}$$

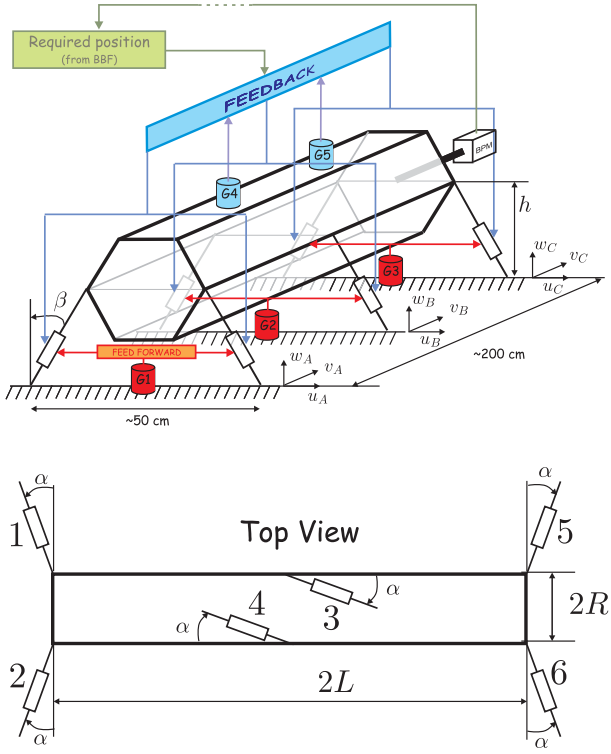

Figure 4. Simplified drawing of the quadrupole.

3.1 Ground motion

In each direction, the coherence of the ground motion between two legs located side by side of the quadrupole is close to one. Thus, it is assumed that the excitation is the same for each pair of legs having the same coordinate along the main quadrupole axis. That is, the excitation vector is $\mathbf{w} = (u_A, v_A, w_A, u_B, v_B, w_B, u_C, v_C, w_C)^T$. Also, the coherence between the ground motion in perpendicular directions is very low. Then, the excitation matrix has the following bloc diagonal form

$$E^T = \begin{pmatrix} \mathbf{1}_1.\mathbf{e}_x & \mathbf{1}_2.\mathbf{e}_x & 0 & 0 & 0 & 0 \\ \mathbf{1}_1.\mathbf{e}_y & \mathbf{1}_2.\mathbf{e}_y & 0 & 0 & 0 & 0 \\ \mathbf{1}_1.\mathbf{e}_z & \mathbf{1}_2.\mathbf{e}_z & 0 & 0 & 0 & 0 \\ 0 & 0 & \mathbf{1}_3.\mathbf{e}_x & \mathbf{1}_4.\mathbf{e}_x & 0 & 0 \\ 0 & 0 & \mathbf{1}_3.\mathbf{e}_y & \mathbf{1}_4.\mathbf{e}_y & 0 & 0 \\ 0 & 0 & \mathbf{1}_3.\mathbf{e}_z & \mathbf{1}_4.\mathbf{e}_z & 0 & 0 \\ 0 & 0 & 0 & 0 & \mathbf{1}_5.\mathbf{e}_x & \mathbf{1}_6.\mathbf{e}_x \\ 0 & 0 & 0 & 0 & \mathbf{1}_5.\mathbf{e}_y & \mathbf{1}_6.\mathbf{e}_y \\ 0 & 0 & 0 & 0 & \mathbf{1}_5.\mathbf{e}_z & \mathbf{1}_6.\mathbf{e}_z \end{pmatrix}$$

Ground vibration measurements have been compared in [17], and led to the choice of a quiet place to perform the stabilization experiments. Figure 5(a) shows the power spectral densities of the ground displacement at that place, and Fig.5(b) shows the coherence between $w_A(t)$ and $w_C(t)$ (located 2 meters apart). Without active control, the stationary response of the quadrupole is given in the Fourier

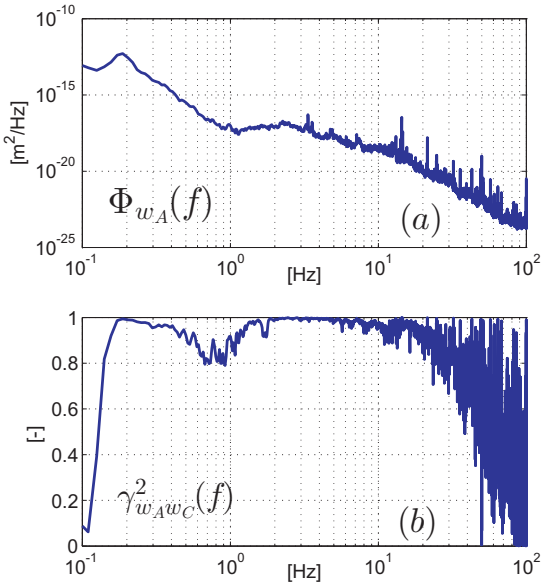

Figure 5. (a) Power spectral density of the ground displacement $\Phi_{w_A}(f)$; (b) Coherence of the vertical displacement between two points $w_A(t)$ and $w_c(t)$.

domain by

$$X(\omega) = T(\omega)W(\omega) \tag{4}$$

where $T(\omega) = [-M\omega^2 + K]^{-1}E$ and the random response is

$$\Phi_x(\omega) = T(\omega)\Phi_w(\omega)T^*(\omega) \tag{5}$$

where $\Phi_w(\omega)$ is the ground excitation matrix [18]. The active control is studied on a single d.o.f. in the next section.

4 Single d.o.f. oscillator

4.1 Modeling

The experimental setup is shown in Fig.6. It consists of a guided piezoelectric stack, clamped in a double membrane like structure to allow only a vertical motion. Two geophones are used to measure the vibrations at both ends of the actuator. The aim of the experiment is to stabilize a small mass laying on the top of the membrane, i.e. the geophone itself.
Assuming that the vertical stiffness of the guide is negligible with respect to the stiffness the actuator, and neglecting the mass of the membrane and actuator, the dynamic equation of the system is

$$m\ddot{x} + k(x - w - \delta) = 0 \tag{6}$$

where m is the mass of the geophone, k the stiffness of the piezoelectric actuator, x the vertical displacement of the geophone on the top of the actuator, w the ground motion, and

$$\delta = nd_{33}V \tag{7}$$

Figure 6. Picture of the experimental setup.

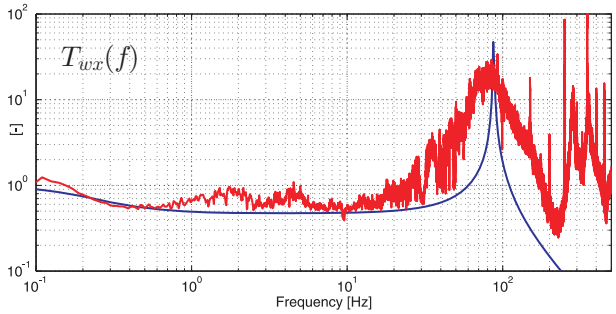

Figure 7. Transfer function $T_{wx}(f)$ calculated, and measured in a quiet environment.

the elongation of the piezoelectric actuator induced by a voltage V [19]. For frequencies below the resonance of the geophone on the stiffness of the actuator, there exists basically two ways to decrease the transfer function $T_{wx}(f)$ between the two geophones: (i) Integrate the signal of the top geophone in a feedback loop:

$$F_b = k\delta = K_p^b x \tag{8}$$

(ii) Integrate the signal of the ground geophone in a feed forward strategy:

$$F_f = k\delta = K_p^f w \tag{9}$$

where K_p^b and K_p^f are the gain of the controllers. Theoretically, both of these strategies are efficient. However, in this study, the first one is preferred because the performances of the feed forward are limited by the coherence between the ground vibration measurement and the actuator. Figure 7 shows the transmissibility $T_{wx}(f)$ using the position feedback strategy. A band pass filter is applied to the control signal between $0.5\ Hz$ and $50\ Hz$. In order to test if the top geophone can be also positioned, the feedback control law has been transformed into a classical Proportional Integral Derivative (PID) controller. Eqs.(8) and (9) become

$$F_b = K_d^b\dot{x} + K_p^b(r - x) + K_i^b\int(r - x)dt \tag{10}$$

$$F_f = K_d^f\dot{w} + K_p^f w \tag{11}$$

where K_d^b, K_i^b, K_d^f are the gains of the controller, and $r(t)$ is the requested position.
Figure 8 shows a short time history simulated with the control law, when the requested position is a square function with an amplitude of $10\ nm$ and steps of $20\ ms$. The following section presents the experimental results obtained for the stabilization.

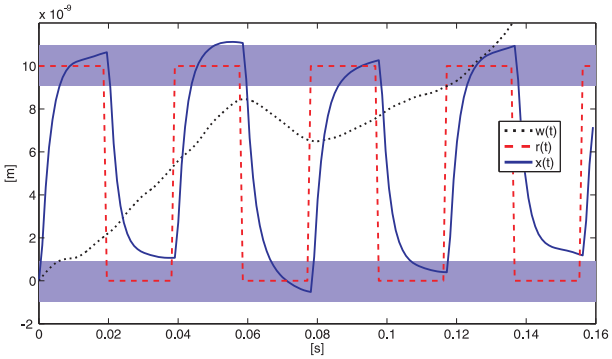

Figure 8. Simulation of the time history of the geophone motion $x(t)$, subjected to a ground excitation $w(t)$ and a requested position $r(t)$.

5 Experiment

The piezo actuator is a $P-753.21C$ [20]. It works in a closed loop configuration together with a built in capacitive sensor and an amplifier (Fig. 9). The calibration factor for the piezo actuator system is $400\ \mu V/nm$. In the closed loop configuration the actuator has a maximum stroke of $25\ \mu m$ and a resolution of $0.1\ nm$. The geophones (Guralp CMG-6T [21]) have a differential sensitivity of about $2000\ V/(m/s)$ and a frequency range between 30 seconds and $100\ Hz$. The real time control system is based on a card $PXI-6289$ [22] for data acquisition. The characteristics of the card are as follows: 32 single ended or 16 differential input channels (18 bit resolution), 4 analog outputs (16 bit resolution).

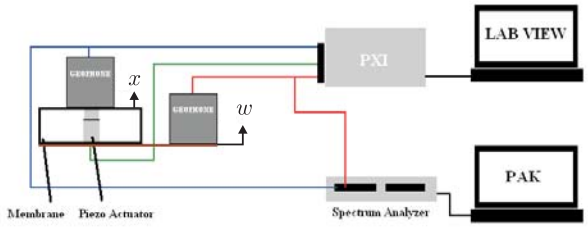

Figure 9. Description of the experimental setup.

A high-pass Butterworth filter with cut-off frequency of $0.1\ Hz$ was applied to the input signal in order to remove its low frequency component, which appears in the signal due to air temperature changes. To avoid membrane excitation at high frequencies, a low-pass Butterworth filter with cutoff frequency of $60\ Hz$ to the output is implemented. The range of the signal for the piezo actuator has the low limit of $-2\ V$. In order to protect the actuator and to ensure that the signal is not exceeding this limit, an offset of $1\ V$ is added to the output signal of the control system. The sampling rate of the card is guaranteed by the producer and can be set up to $625\ kSample/s$. On the other hand, the program loop rate can vary depending on many factors (CPU load, amount of calculations in the loop, amount of information to be updated during the loop run). These two processes have to be well synchronized. In order to evaluate the performances of the stabilization, the geophones signal are sent to a second acquisition system in parallel with the PXI. This system has a better resolution, and better performances are delivered by the PXI when it does not save data. The system used was the MKII made by Müller-BBM. It contains 16 input channels with DSP (Digital Spectrum Processing) for each four channels with a sampling frequency up to $204\ kHz$. The dynamic resolution is 24 bits, and it can be used in a range between $10\ mV$ and $50\ V$ with a noise level lower than $1pV$. The transfer function $T_{wx}(f)$ is compared with the theoretical curve in Fig.7. It has been calculated as

$$T_{wx}(f) = \sqrt{\frac{\Phi_x(f)}{\Phi_w(f)}} \tag{12}$$

Figure 10 shows the RMS integrated displacement calculated from $\Phi_w(f)$ and $\Phi_x(f)$. At $1\ Hz$, one sees that the feedback control has reduced $\sigma_x(f)$ from $2\ nm$ down to $1.2\ nm$. This value is close to the requirements (Fig.1(a)).

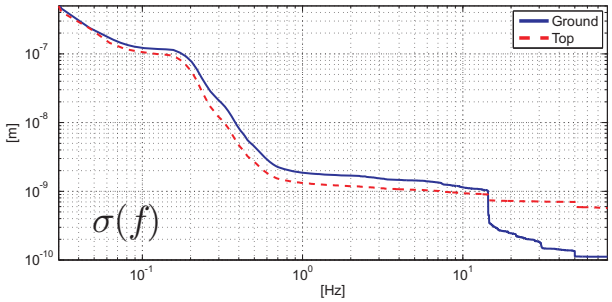

Figure 10. RMS integrated of the ground displacement $\sigma_w(f)$ and the top displacement $\sigma_x(f)$.

Better results are expected from an optimized combination of the feedback and feed forward, and a more adapted hardware.

6 Conclusions and future work

First of all, some key experiments of quadrupole stabilization have been compared. In order to fulfil both the stabi-

lization and positioning requirements, it has been chosen to mount the structure on stiff supports. Then, a concept of six legs derived from a Stewart platform has been presented. The stabilization and positioning strategies have been studied on a single d.o.f. system. Finally, the stabilization has been validated experimentally in a quiet environment. This experiment has shown that the transfer function between the two geophones can be divided by nearly a factor two. The RMS integrated of the mass has been reduced at $1.2\ nm$ at $1\ Hz$, showing also that the geophone is capable to measure low frequency vibrations with amplitudes close to the nanometer.
Before stabilizing and positioning experimentally the long quadrupole, the next step will be to consider first a heavy compact objet, in order to address all the difficulties of the stabilization and positioning of the long quadrupole (except its flexibility), which are mainly load compensation, jointure design, control optimization.

References

[1] G. Riddone, D. Schulte, H. Mainaud-Durand, I. Syratchev, W. Wuensch, R. Zennaro, R. Nousiainen, and A. Samoshkin. Technical specification for the CLIC two-beam module. In *Proceedings of the EPAC 08, Geona (Italy).*, 2008.

[2] http://clic-stability.web.cern.ch/clic-stability/.

[3] D. Schulte. Beam based alignment in the new clic main linac. In *Proceedings of the 2009 Particle Accelerator Conference, Vancouver, Canada*, 2009.

[4] A. Stochino, B. Abbot, Y. Aso, M. Barton, A. Bertolini, V. Boschi, D. Coyne, R. DeSalvo, C. Galli, Y. Huang, A. Ivanov, S. Marka, D. Ottaway, V. Sannibale, C. Vanni, H. Yamamoto, and S. Yoshida. The Seismic Attenuation System (SAS) for the advanced LIGO gravitational wave interferometric detectors. *Nuclear Instruments and Methods in Physics Research A*, 598:737–753, 2009.

[5] A. Carter, G. King, T. Ulrich, W. Hasley, D. Alchenberger, and T. Perkins. Stabilization of an optical microscope to 0.1 nm in the three dimensions. *Applied Optics*, 46(3):421–427, 2007.

[6] K. Furutani, M. Suzuki, and R. Kudoh. Nanometer cutting machine using a Stewart-platform parallel mechanism. *Measurement Science and Technology*, 15:467–474, 2004.

[7] C. Montag. Active stabilization of mechanical quadrupole vibrations for linear collider. *Nuclear Instruments and Methods in Physics Research A*, 378:396–375, 1996.

[8] C. Montag. *Active Stabilization of Mechanical Quadrupole Vibrations in a Linear Collider Test Facility*. PhD thesis, Hamburg University, 1996.

[9] S. Redaelli. *Stabilization of Nanometer-Size Paricle Beams in the Final focus System of the Compact LInear Collider CLIC*. PhD thesis, University of Lausanne, 2004.

[10] B. Bolzon. *Etude des vibrations et de la stabilisation l'chelle sous-nanomtreique des doublets finaux d'un collisionneur linaire*. PhD thesis, University of Savoie, 2007.

[11] S. Allison, L. Eriksson, L. Hendrickson, T. Himel, and A. Seryi. Active vibration suppression r+d for the next linear collider. In *Proceedings of the Particle Accelerator Conference, Chicago*, 2001.

[12] J. Frisch, A. Chang, V. Decker, E. Doyle, L. Eriksson, L. Hendrickson, T. Himel, T. Markiewicz, R. Partidge, and A. Seryi. Vibration stabilization of a mechanical model of a x-band linear collider final focul magnet. In *22nd International Linear Collider Conference, 16-18 August (Germany)*, 2004.

[13] K. Artoos, O. Capatina, C. Collette, M. Guinchard, C. Hauviller, F. Lackner, J. Pfingstner, H. Schmickler, M. Sylte, M. Fontaine, B. Bolzon, L. Brunetti, G. Deleglise, N. Geoffroy, and A. Jeremie. Study of the stabilization to the nanometre level of mechanical vibrations of the CLIC main beam quadrupoles. In *Proceedings of the 2009 Particle Accelerator Conference, Vancouver, Canada*, 2009.

[14] J. Spanos, Z. Rahman, and G. Blackwood. A soft 6-axis active vibration isolator. In *Proceedings of the American Control Conference, Seatle, Washington.*, 1995.

[15] A. Hanieh. *Active Isolation and damping of Vibrations via Stewart Plateform*. PhD thesis, University of Brussels, 2004.

[16] A. Preumont. *Vibration Control of Active Structures, An Introduction*. Kluwer Academic Publishers, 2002.

[17] K. Artoos, O. Capatina, C. Collette, M. Guinchard, C. Hauviller, M. Sylte, B. Bolzon, and A. Jeremie. Ground vibration and coherence length measurements for the CLIC nano-stabilization studies. In *Proceedings of the 2009 Particle Accelerator Conference, Vancouver, Canada*, 2009.

[18] A. Preumont. *Random Vibration and Spectral Analysis*. Kluwer Academic Publishers, 1994.

[19] A. Preumont. *Mechatronics, Dynamics of Electromechanical and Piezoelectric Systems*. Springer, 2006.

[20] Physik Instruments. Physik instruments catalogue.

[21] Guralp. Guralp catalogue.

[22] National Instruments. National instruments catalogue.